

Multiscale Feature Importance-based Bit Allocation for End-to-End Feature Coding for Machines

JUNLE LIU, School of Electronics and Communication Engineering, Sun Yat-Sen University, China
YUN ZHANG, School of Electronics and Communication Engineering, Sun Yat-Sen University, China
ZIXI GUO, School of Electronics and Communication Engineering, Sun Yat-Sen University, China
XIAOXIA HUANG, School of Electronics and Communication Engineering, Sun Yat-Sen University, China
GANGYI JIANG, Faculty of Information and Science and Engineering, Ningbo University, China

Feature Coding for Machines (FCM) aims to compress intermediate features effectively for remote intelligent analytics, which is crucial for future intelligent visual applications. In this paper, we propose a Multiscale Feature Importance-based Bit Allocation (MFIBA) for end-to-end FCM. First, we find that the importance of features for machine vision tasks varies with the scales, object size, and image instances. Based on this finding, we propose a Multiscale Feature Importance Prediction (MFIP) module to predict the importance weight for each scale of features. Secondly, we propose a task loss-rate model to establish the relationship between the task accuracy losses of using compressed features and the bitrate of encoding these features. Finally, we develop a MFIBA for end-to-end FCM, which is able to assign coding bits of multiscale features more reasonably based on their importance. Experimental results demonstrate that when combined with a retained Efficient Learned Image Compression (ELIC), the proposed MFIBA achieves an average of 38.202% bitrate savings in object detection compared to the anchor ELIC. Moreover, the proposed MFIBA achieves an average of 17.212% and 36.492% feature bitrate savings for instance segmentation and keypoint detection, respectively. When the proposed MFIBA is applied to the LIC-TCM, it achieves an average of 18.103%, 19.866% and 19.597% bit rate savings on three machine vision tasks, respectively, which validates the proposed MFIBA has good generalizability and adaptability to different machine vision tasks and FCM base codecs.

CCS Concepts: • **Computing methodologies** → **Image compression**; *Computer vision*; • **Information systems** → Data encoding and canonicalization.

Additional Key Words and Phrases: Feature coding for machines, deep learning, image coding, bit allocation, object detection

ACM Reference Format:

Junle Liu, Yun Zhang, Zixi Guo, Xiaoxia Huang, and Gangyi Jiang. 2024. Multiscale Feature Importance-based Bit Allocation for End-to-End Feature Coding for Machines. *ACM Trans. Multimedia Comput. Commun. Appl.* x, x, Article XXX (October 2024), 19 pages. <https://doi.org/XXXXXXXX.XXXXXXX>

Authors' Contact Information: Junle Liu, liujle@mail2.sysu.edu.cn, School of Electronics and Communication Engineering, Sun Yat-Sen University, Shenzhen, Guangdong, China; Yun Zhang, zhangyun2@mail.sysu.edu.cn, School of Electronics and Communication Engineering, Sun Yat-Sen University, Shenzhen, Guangdong, China; Zixi Guo, guozx29@mail2.sysu.edu.cn, School of Electronics and Communication Engineering, Sun Yat-Sen University, Shenzhen, Guangdong, China; Xiaoxia Huang, huangxiaoxia@mail.sysu.edu.cn, School of Electronics and Communication Engineering, Sun Yat-Sen University, Shenzhen, Guangdong, China; Gangyi Jiang, jianggangyi@nbu.edu.cn, Faculty of Information and Science and Engineering, Ningbo University, Ningbo, Zhejiang, China.

Permission to make digital or hard copies of all or part of this work for personal or classroom use is granted without fee provided that copies are not made or distributed for profit or commercial advantage and that copies bear this notice and the full citation on the first page. Copyrights for components of this work owned by others than the author(s) must be honored. Abstracting with credit is permitted. To copy otherwise, or republish, to post on servers or to redistribute to lists, requires prior specific permission and/or a fee. Request permissions from permissions@acm.org.

© 2024 Copyright held by the owner/author(s). Publication rights licensed to ACM.

ACM 1551-6865/2024/10-ARTXXX

<https://doi.org/XXXXXXXX.XXXXXXX>

1 Introduction

In recent years, the technical advancement and wide applications of multimedia have led to exponential growth in the volume of images and videos. With the rapid development of artificial intelligence, the processing of images and videos is shifting from viewed and hand-crafted with manpower to automatically analyzed by deep machine vision models. In the future, a significant portion of image and video content will be automatically processed by intelligent machine vision models as end users, rather than being viewed by humans.

Conventional image and video compression methods were primarily designed for human vision by exploiting signal and visual redundancies, such as JPEG and BPG for image, and High Efficiency Video Coding (HEVC) and Versatile Video Coding (VVC) [4] for video. These methods primarily focus on human visual mechanisms while neglecting machine visual mechanisms. Consequently, the performance of the downstream machine tasks can hardly be maintained by simply using compressed images / videos from human vision oriented image / video codecs. To adapt future intelligent visual analytics and applications, expert groups proposed new standards such as Image/Video Coding for Machines (ICM/VCM) [30] and Joint Photographic Experts Group with Artificial Intelligence (JPEG-AI) [2], which have attracted significant attention [16]. As highlighted in [14], [18] and [44], the goals of image compression for human vision differ substantially from those for machine vision models. These initiatives [15] emphasized the importance of addressing machine vision-specific compression, which will become an essential component of future codecs. In Compress-Then-Analyze (CTA) framework [14], compressed images shall be reconstructed and then input for analysis. It is simple and compatible with existing image communication system, but it costs decoding overhead at the client. In Analyze-Then-Compress (ATC) paradigm [14], only analytical results are required to be compressed and transmitted, which are able to achieve an extremely high compression ratio. However, ATC schemes are usually task-specific and have low generalizability or efficiency to unknown machine tasks.

A number of ICM/VCM work have been developed based on conventional image/video coding framework. Chamain *et al.* [5] connected a machine vision task network to the decoder and trained it jointly with the codec during training. Yang *et al.* [39] proposed to transmit the contour and color components of face images separately for face recognition tasks. Wang *et al.* [36] optimized the object detection network to adapt to images with different losses at various bit rates. Wang *et al.* [35] proposed an end-to-end compression with offline optimization using the Lagrange multiplier in the loss function for machine vision. Le *et al.* [24] proposed a machine vision task network trained on uncompressed images to finetune the jointly trained machine vision task network and codec. In addition, optimization methods for bit rate allocation and quantization maps were explored. Huang *et al.* [23] proposed a Region-of-Interest for Machines (ROIM) based bit allocation optimization algorithm for object detection. It first detected image regions sensitive to the detection task using an object detection model and then allocated more bit streams to these sensitive regions. Choi *et al.* [10] trained a network to generate an image quantization allocation map and then performed JPEG compression on the quantized image. Cui *et al.* [12] proposed an image compression sensing coding framework using local structural sampling to reconstruct images. However, these optimizations were performed based on traditional image/video codecs that were originally designed for human vision, which may degrade machine vision accuracy.

To improve ICM/VCM coding efficiency, adaptations to machine vision tasks were performed on Learned Image Compression (LIC) models [19, 27] for high compression efficiency. Shindo *et al.* [32] used regions of interest for machine vision as masks to assist the image encoding. Zhang *et al.* [43] decomposed images into semantic, structural, and signal layers to achieve variable-length encoding for machine vision. Chen *et al.* [7] employed prompt finetuning to adapt end-to-end image

compression into machine vision-oriented codecs. Although these methods improved machine vision tasks for traditional image encoders, they still require reconstructing the image at decoder side, which not only introduces additional computational overhead but also needs to transmit an additional bit cost of image reconstruction information that may not be required in machine vision tasks. However, compressing and reconstructing signal level images brings computational overhead. In addition, the compression ratio could be improved as machine vision properties were not fully exploited.

Another ICM/VCM paradigm is encoding the features extracted from images and directly performing the machine vision tasks based on the decoded features, which is newly called Feature Coding for Machines (FCM). Alvar *et al.* [1] proposed a multitask joint training method for task networks and codecs. Hyomin *et al.* [9] [8] split the features, with one part used for machine vision tasks and the others used as enhanced features for image reconstruction. Zhang *et al.* [42] proposed a similar unified and scalable image compression framework for humans and machines which jointly optimizes the network in end-to-end manner. Tu *et al.* [33] proposed a FCM by transferring knowledge from the pixel domain to the compressed domain to improve compression performance. Özyılkan *et al.* [45] extracted intermediate deep features from original images and used them to generate task-specific features during feature division. In [26], after extracting features from the image, a gate module was used on the encoding side to filter task-specific features. After compression, the back-end network adapted and transformed these features to perform tasks. Wang *et al.* [37] extracted features relied upon machine vision tasks from images, and the encoding side preliminarily reconstructed a rough image based on these features, transmitted the image residuals, then simultaneously performed machine vision tasks and image reconstruction at the decoding side. In [3], the encoder extracted and compressed image features, while the decoding side used a Transformer-based task network and an image reconstruction network. Wang *et al.* [34] proposed a teacher-student model which used a low bit-rate decoder to assist the high bit-rate decoder in decoding, achieving multi-granularity feature compression. Codevilla *et al.* [11] converted the encoded latent space representations into task-adapted features through super-resolution and feature transformation modules. In [17], self-supervised learning was adopted to extract general features, which were then encoded, transmitted, and converted into features suitable for various machine vision tasks. Hu *et al.* [22] proposed a bit allocation method that utilized the sensitivity of feature channels, named the Sensitivity-Aware Bit Allocation (SABA) method. Yang *et al.* [40] experimentally validated that compressing features were more effective than compressing images. These methods compress and reconstruct features directly, avoiding the distortion caused by the image-level reconstruction. The FCM paradigm is superior to direct ICM. From an information theory perspective, the FCM paradigm first extracts features from images and then leverages the prior knowledge of the feature extraction model to eliminate redundant information which is irrelevant to machine vision tasks. Additionally, FCM has advantages of information encryption and low complexity by removing image reconstruction.

Complex deep vision task models generally require multiscale features in the decision-making process. In this case, compressing these multiscale features becomes indispensable for remote intelligent visual analytics. Liu *et al.* [28] developed a scalable feature coding model by gradually coding and transmitting features from shallower networks, which have lower-level features and more complete information. Ning *et al.* [38] hierarchically extracted semantic features from fine-grained to coarse-grained, where the encoded features were gradually enhanced. The features for encoding and transmission were selected based on the specified target tasks in remote applications. However, these approaches could not comprehensively plan the overall features to achieve the best performance. In addition, it may include redundancies or features that are irrelevant to the task when transmitting enhanced features. In [29], only part of the features of the pyramid structure

was compressed, and all scales of features were reconstructed using the transmitted partial-scale features. However, the predicted features might introduce errors due to the inaccuracy of the predictive model and cumulative feature errors in transmitted features after encoding and decoding, which can affect the performance of the machine vision model. In multiscale FCM, feature attributes and their dependences on machine vision tasks could be further exploited for better generalizability. The importance differences of the multiscale features and inter-scale correlations could be further exploited for higher efficiency.

In this paper, we propose a Multiscale Feature Importance-based Bit Allocation (MFIBA) for end-to-end FCM, which significantly improves feature coding efficiency while maintaining the accuracies of multiple machine tasks. The key contributions are

- We experimentally analyze the visual importance of multiscale features in machine vision tasks and propose a Multiscale Feature Importance Prediction (MFIP) to predict the importance of each scale of features.
- We propose a task loss-rate model for multiscale feature, which accurately models the relationship between task loss from compression and feature coding bits.
- We propose a Multiscale Feature Importance-based Bit Allocation (MFIBA) for FCM by exploiting the feature importance differences among scales, which reduces the feature coding bits while maintaining the accuracies of three machine vision tasks.

The paper is organized as follows: Section II formulates the problem of FCM and statistically analyzes feature importance. Section III presents the proposed MFIBA methods for FCM. Section IV presents the experimental results and analysis. Section V concludes the paper.

2 Problem Formulation and Statistical Analysis

In remote intelligent visual applications, the features of edge visual sensors are required to be coded and transmitted to remote data centers for visual analytics. The performance of machine vision tasks rely on the quality of the image feature. FCM is to code the feature effectively while maintaining the feature quality. The FCM objective is

$$\min D(\mathbf{F}, \mathbf{F}'), \quad \text{s.t. } R(\mathbf{F}) < R, \quad (1)$$

where \mathbf{F} and \mathbf{F}' represent the original features and reconstructed features from decoding, $D(\mathbf{F}, \mathbf{F}')$ is a distortion metric that measures the features quality difference and the impacts to machine vision tasks, $R(\mathbf{F})$ denotes the coding bit rate for the features \mathbf{F} .

Many deep networks of machine vision recommended by the VCM standard involve multiscale features, such as Faster Region-based Convolutional Network (R-CNN) [31] and RetinaNet [25] for object detection, Keypoint R-CNN [13] for keypoint detection, and Mask R-CNN [20] for semantic segmentation and instance segmentation. However, features at different scales are not important equivalently. To verify this assumption, we added distortions to the multiscale features (scale $0, 1, \dots, n, P$) and analyzed their impacts on object detection. We used the ResNet50 Feature Pyramid Network (FPN) [21] as backbone to extract features at five different scales. By applying various levels of compression noise from ELIC [19] to each scale separately and categorizing the detection targets into three categories (large, medium, and small) following the definition of COCO2017 dataset, we analyzed the relationship between features at different scales and target sizes on the COCO2017 validation dataset for the object detection.

Fig. 1 shows object detection results of replacing one scale of feature with the coded one at different bit rates, where the horizontal axis represents the bit rate, and the vertical axis represents the accuracy of the object detection. As shown in Fig. 1, the accuracies increase as the feature are compressed with higher bit rate. However, the accuracies vary with the scales and object sizes.

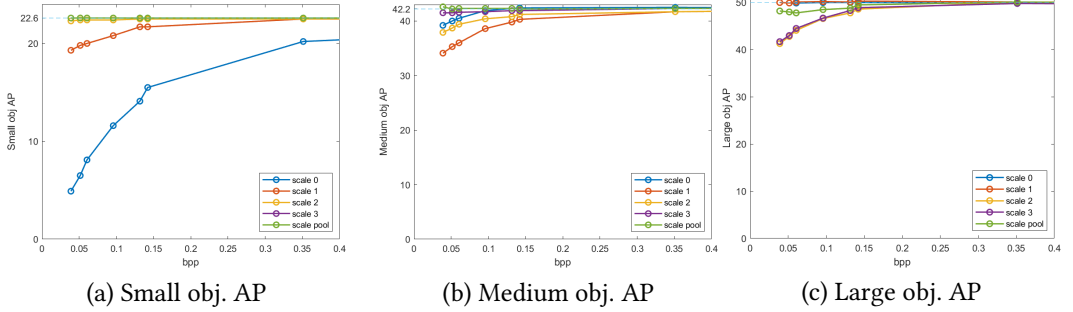


Fig. 1. Object detection accuracies of using compressed features at different scales (following COCO2017 dataset definition) and bit rates. (a) Small objects (b) Medium objects (c) Large objects.

From Fig. 1(a), the accuracy degrades significantly while compressing features at scale 0 for small objects, while the accuracies degrade more significantly for scale 1 and scale 3 for medium and large objects. It is found that small objects are more sensitive to the compression distortion of larger-scale features, such as scale 0, compared to smaller-scale features. In contrast, large objects are more sensitive to the distortion of smaller-scale features, such as scale 3 and scale pool. This is because feature receptive fields vary at different scales, larger-scale features have smaller receptive fields, making them capable of detecting small objects, but less effective at discovering large objects. Smaller-scale features aggregate information from larger receptive fields, making them capable of detecting large objects, but less sensitive to small objects. Therefore, different sizes of objects depend on features from different scales. Overall, it is found that the feature importance varies with the scales and target object sizes, which shall be exploited in FCM.

To achieve better machine vision tasks under bit rate constraints, it is essential to allocate more bits to the more important features. Thus, we shall assign reasonable weights to features of varying scales, indicating that their impact on the task differs after compression losses. The objective of MFIBA is formulated as

$$\min \sum_i w_i L(\mathbf{F}_i, \mathbf{F}'_i), \quad s.t. R(\mathbf{F}_i) < R_T, \quad (2)$$

where $i \in \{0, 1, \dots, n, P\}$ denotes the i -th scaled feature, n is the number of scales for features, P is a pooling feature from the n scale of features. w_i is the weight assigned to each scaled feature i , which depends on the instance image and task. We predict these weights in the proposed MFIBA model. \mathbf{F}_i and \mathbf{F}'_i are the original features and compressed features, $L(\mathbf{F}_i, \mathbf{F}'_i)$ denotes the distortion loss after feature compression, $R(\mathbf{F}_i)$ is the coding bit rate of \mathbf{F}_i , R_T is a target bit rate.

3 Proposed MFIBA for FCM

To compress the multiscale features more effectively, we propose a MFIBA for FCM by considering the importance differences of multiscale features. Fig. 2 shows the framework of proposed MFIBA for FCM. A feature extraction network is used to extract deep features for machine vision tasks. In this paper, we select the commonly employed ResNet50-FPN [21] as the feature extraction network for tasks, including object detection, keypoint detection, and instance segmentation. While doing the machine vision tasks, all scales of features participate in the decision-making, which requires to code and transmit features of all scales to remote intelligent data processing center.

To improve the compression efficiency of FCM, we proposed MFIBA to assign the feature coding bits more reasonably based on the importance of the feature, which includes offline and online

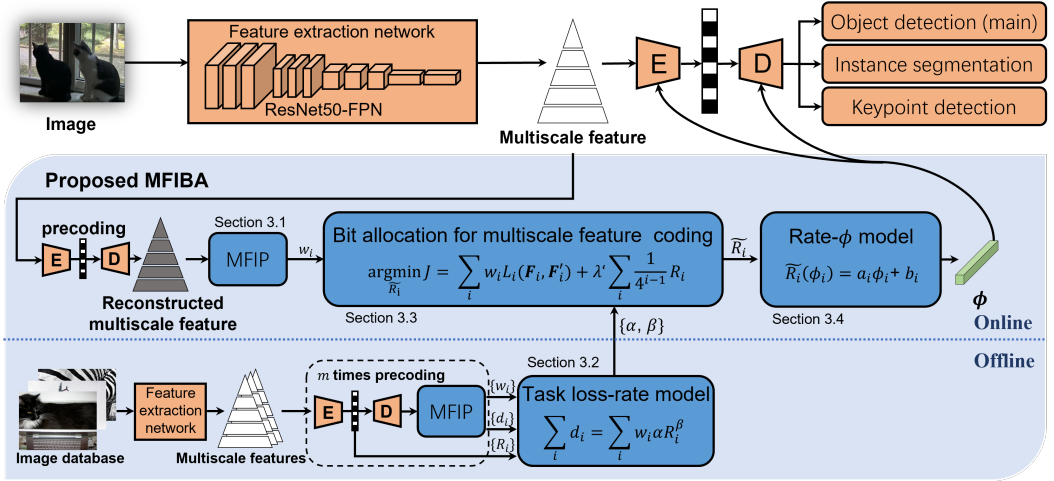


Fig. 2. Framework of the proposed MFIBA for FCM.

phases. In offline phase, multiscale feature maps extracted from the image database. Then, feature importance weights $\{w_i\}$ and task losses $\{d_i\}$ from Multiscale Feature Importance Prediction (MFIP) and bit rates $\{R_i\}$ from codec multi-pass coding are input to establish a task loss-rate model. Then, in the online phase, the multiscale features are first precoded and importance weights are predicted through the MFIP. Then, based on online $\{w_i\}$ and offline task loss-rate model, bit allocation algorithm is developed to determine the budget bit rate for each scale of feature. Finally, rate- ϕ model is used to map the rate to the hyperparameter of learned feature codec for coding control.

3.1 MFIP Module

Based on the observations in Section II, multiscale feature shall be given different importance. To measure and predict the importance of each feature scale, we propose MFIP module for each instance image, as shown in Fig. 3. First, we precode multiscale features at different quality levels. Then, the MFIP module combines the precoded results with the original features, replacing some scales of the original features with the precoded features. The recombined features are put in the task heads [31] to obtain detection results of different scales and distortions. These results are compared with the detection results of using lossless multiscale features to derive loss vectors of each feature scale at different quality levels. Considering the different dynamic ranges of these losses, these loss vectors are normalized. Then, the task loss for each scale feature at different qualities is averaged to get the average loss d_i . Finally, the importance weights of multiscale features are predicted from the average of normalized task losses.

Since object detection task loss is the final metric to optimize, we believe that there is a high correlation between the importance weights of the features and the average loss values in Fig.3. To analyze this correlation, the weights can be expressed as $\hat{w}_i = f(d_i)$, where d_i is the task accuracy loss of i -th scale feature, \hat{w}_i is the predicted weight and $f(\cdot)$ is the mapping function. To investigate the relationship between weights w_i and task losses d_i , we visualize their correlation across images from the COCO 2017 validation dataset in Fig. 4. We can observe that there is a high linear correlation between them. For simplicity, we predict \hat{w}_i directly with d_i , which is expressed as $\hat{w}_i = d_i$.

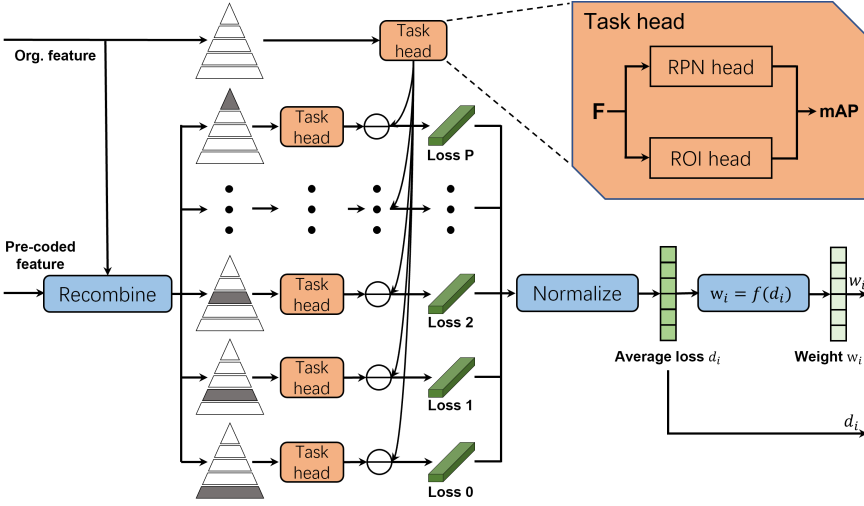


Fig. 3. Flowchart of the proposed MFIP module.

If more computational resources are available, we can employ a line search method to find the optimal w_i . Since loss d_i is continuous, it is challenging to find the optimal w_i directly. The search mainly includes four key steps: 1) we first discretize d_i as an initial prediction of the weights \hat{w}_i . 2) We apply the line search method starting from the initial \hat{w}_i . Specifically, for each scale feature, we quantize \hat{w}_i to two decimals and perform the rate allocation in the MFIBA using two calibrated weights, i.e., $\hat{w}_i + 0.01$ and $\hat{w}_i - 0.01$. 3) The compression efficiency is evaluated based on the object detection accuracy from compressed features and coding bit rate. If better compression efficiency is achieved by using either $\hat{w}_i + 0.01$ or $\hat{w}_i - 0.01$. Then, an additional step, $\hat{w}_i + 0.02$ or $\hat{w}_i - 0.02$ will be searched and compared. 4) Steps 2)-3) are repeated until the optimal importance weight for each scale is found. Therefore, the MFIBA algorithm can allocate bitrates more effectively to different scale features, achieving better compression performance on object detection.

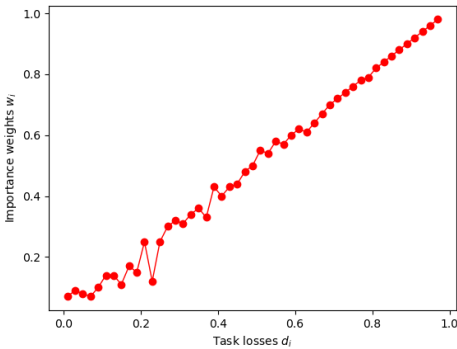


Fig. 4. Relationship between task loss d_i and importance weight w_i across all images.

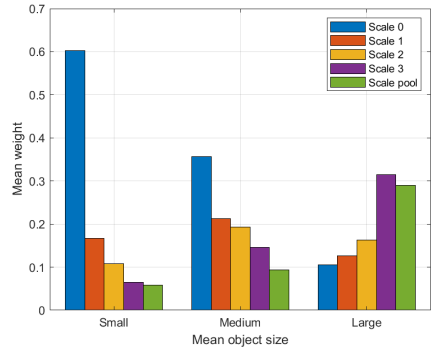


Fig. 5. Relationship between the object target sizes and the average weight \hat{w}_i .

Table 1. CC and RMSE of the task loss-rate models, where the best are in bold.

Task loss-rate models	Evaluation metrics	mAP@50:95	mAP@75
Quadratic	CC	0.9956	0.9930
	RMSE	1.0078	1.5966
Cauchy-distributed	CC	0.9991	0.9989
	RMSE	0.4551	0.6217

Furthermore, we analyzed the relationship between the feature weights \hat{w}_i calculated by the MFIP module and different object sizes in the images. The statistical results are shown in Fig. 5. It can be observed that in images with smaller average target sizes, the average weight of larger-scale features is higher, while in images with larger average target sizes, the weights are more inclined towards smaller-scale features. Thus, the MFIP module effectively allocates feature weights based on target sizes. Notably, the inherent similarities in the underlying mechanisms of machine vision tasks suggest that importance weights can be generalized to tasks beyond object detection [18].

3.2 Task Loss-Rate Model

To model the relationship between task loss and bit rate, we propose a feature importance weighted task loss-rate model based on the Cauchy-distributed Rate-Distortion (RD) model [41]. Due to the varying importance of multiscale features in machine vision tasks, we predicted the importance of each scale of features w_i using the MFIP module. Then, the machine vision task loss-rate model is constructed from the predicted feature weights and the feature distortions, which can be modeled by the exponential model [41]. Therefore, the task loss-rate model can be presented as

$$\sum_i d_i = \sum_i w_i \alpha R_i^{-\beta}, \quad (3)$$

where R_i is the bit rate for compressing features at the i^{th} scale, w_i is the weights of multiscale features, d_i is the task loss obtained from the MFIP module, α and β are factors for the Cauchy-distributed loss-rate model, which are derived from offline multi-pass precoding of feature dataset.

To evaluate the accuracy of Cauchy-distributed loss-rate model, we performed coding experiments for multiscale features of all images in the COCO2017 validation dataset, where used as the base codec. Object detection using Faster R-CNN was performed by using the reconstructed features from different coding bit rates. The detection accuracy was measured with mAP@50:95 and mAP@75. Fig. 6 presents the fitting results of the Cauchy-distributed task loss-rate model in Eq. 3 and quadratic task loss-rate model [6] for comparison, where y-axis represents loss in object detection accuracy on mAP@50:95 and mAP@75, and x-axis represents bit rate in bpp. We can observe that the model fits the real data better. The fitting accuracies of the models are illustrated in Table 1. The Correlate Coefficients (CC) of the cauchy-distributed task loss-rate model in mAP@50:95 and mAP@75 are 0.9991 and 0.9989, respectively, which are higher than those of quadratic model. The Root Mean Squared Error (RMSE) in mAP@50:95 and mAP@75 are 0.4551 and 0.6217, respectively, which are lower than those of the quadratic task loss-rate model. It shows that the Cauchy-distributed task loss-rate model can accurately model the relationship between task loss and rate. In addition, the accurate loss-rate model will consequently improve the bit allocation accuracy in MFIBA.

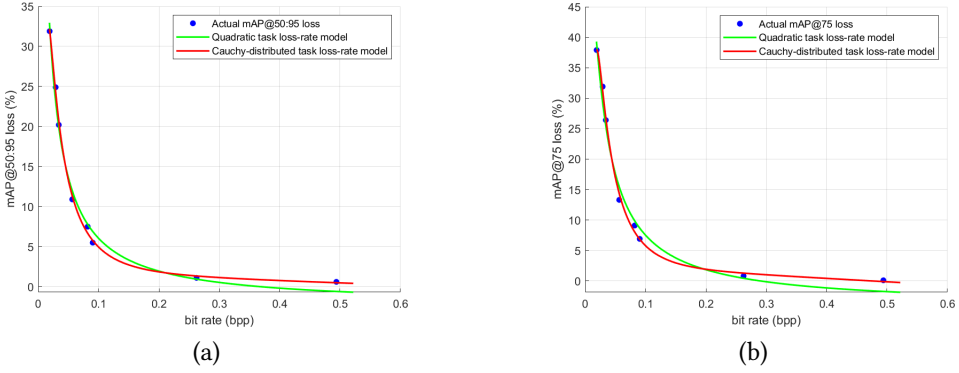


Fig. 6. Relationship between task loss and bit rate, (a) mAP@50:95, (b) mAP@75.

3.3 Bit Allocation for Multiscale Feature Coding

Based on the predicted feature importance weights \hat{w}_i and the introduced Lagrange Multiplier λ , the objective function in Eq. 2 can be updated by minimizing a loss function J as

$$J = \sum_i \hat{w}_i L_i(\mathbf{F}_i, \mathbf{F}'_i) + \lambda \sum_i R_i \quad (4)$$

where $L_i(\mathbf{F}_i, \mathbf{F}'_i)$ is the distortion loss of the i -th scale feature, R_i is the bit rate of encoding i -th scale feature. $i \in \{0, 1, \dots, n, P\}$ denotes the i -th scale of feature, n is the number of feature scales and P denotes the pooling feature. Note that for low complexity, \hat{w}_i is a predicted version of w_i by using the MFIP module in Section 3.1. Considering the different sizes of feature maps across various scales, let S_0 be the size of the 0-th feature map, since the compression rate R_i is based on the size of each scale of feature, the bit rate of the overall objective function is based on the sum of bits across all scales of features, the final optimization objective is updated as

$$J = \sum_i \hat{w}_i L_i(\mathbf{F}_i, \mathbf{F}'_i) + \lambda' \sum_i \frac{1}{k^i} R_i \quad (5)$$

where $\lambda' = \lambda S_0$, k is a scaling ratio of features between scales i and $i + 1$, k is 4 for ResNet50-FPN.

Applying Eq. 3 to Eq. 5, it is easy to prove that Eq. 5 is convex. So we can get the optimal solution by calculating the partial derivative of each variable with respect to the optimization function. By setting the partial derivatives to zero, the optimal budget rate \tilde{R}_i for i^{th} scale feature can be determined as

$$\tilde{R}_i = \left(\frac{\hat{w}_i \alpha \beta}{\lambda' / k^i} \right)^{\frac{1}{\beta+1}}, \quad (6)$$

where $i \in \{0, 1, \dots, n, P\}$, \hat{w}_i is the predicted weights obtained from MFIP module. Based on this solution, it is found that the bit budget \tilde{R}_i of i^{th} scale feature increases as the feature importance \hat{w}_i increases, and vice versa.

3.4 Rate- ϕ Model for End-to-end Feature Coding

Since the feature codecs were based on the end-to-end image codecs, the coding bit rate was controlled by the hyperparameter ϕ within the compression network. In end-to-end LIC network, the loss function is conventionally formulated as $L = R + \phi D$, where ϕ serves as the Lagrange multiplier balancing the trade-off between the distortion loss D and the rate R . In end-to-end LIC

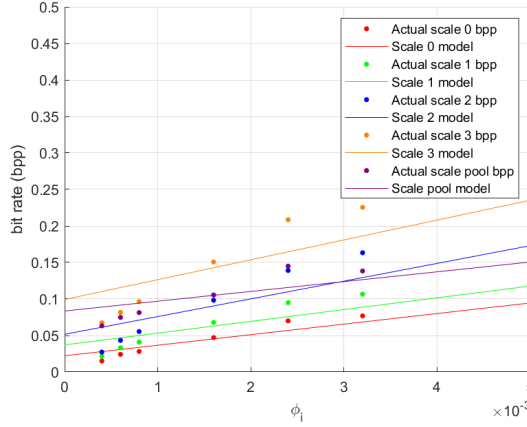
Table 2. CC and RMSE of the $R_i(\phi_i)$ model.

Feature scale	0	1	2	3	P
CC	0.9938	0.9855	0.9823	0.9774	0.9768
RMSE	0.0084	0.0145	0.0238	0.0321	0.0181

codecs, the bit budget \widetilde{R}_i cannot be applied to the end-to-end LIC codecs for coding control directly, but to be converted to the multiplier ϕ . To this end, Rate- ϕ model is developed to establishes an explicit mapping between ϕ and R_i , $\phi = \{\phi_0, \phi_1, \dots, \phi_n, \phi_P\}$, and R_i is the coding rate of different feature scales. In this work, we model the relationship between the bit rate R_i and ϕ_i with a linear function, which can be expressed as

$$R_i(\phi_i) = a_i \times \phi_i + b_i, \quad (7)$$

where a_i and b_i are weighting factors of scale i .

Fig. 7. Relationship between the bit rate $R_i(\phi_i)$ and ϕ_i .

To testify the accuracy of Eq. 7, we experimentally analyzed the $R_i(\phi_i)$ function while coding each scale of feature. Fig. 7 shows the relationship between $R_i(\phi_i)$ and ϕ_i from feature coding, where dots are from real coded features from COCO2017 and the lines are fitted curves using Eq. 7. The lines generally fit well with the collected data for multiscale features. Table 2 accuracies in terms of CC and RMSE of fitted results by using Eq. 7, where P stands for the pooling feature from multiscale features. The CC between the actual coding bit rate and the $R_i(\phi_i)$ model of the five scaled features are 0.9938, 0.9855, 0.9823, 0.9774, and 0.9768, respectively. The RMSE of them are 0.0084, 0.0145, 0.0238, 0.0321, and 0.0181, respectively. It can be observed that the $R_i(\phi_i)$ function effectively and accurately captured the relationship between the hyperparameter ϕ and the resulting coding bit rate, demonstrating its ability to precisely model how changes in ϕ influence compression dynamics.

Finally, based on feature bit budget \widetilde{R}_i and Eq. 7, hyperparameter ϕ_i for i^{th} feature coding control is obtained as

$$\phi_i = (\widetilde{R}_i - b_i)/a_i. \quad (8)$$

By implementing Eq. 8, the MFIBA enables a more efficient feature bit allocation for FCM.

Table 3. BDBR of the proposed MFIBA+ELIC and benchmark schemes compared to ELIC on object detection. [Unit:%].

Coding Schemes	mAP@50:95	mAP@75
SABA [22]+ELIC	2.113	6.073
VTM 17.0 [4]	-5.661	-18.625
Retrained ELIC	-13.477	-14.179
MFIBA+ELIC	-16.118	-21.586
Finetuned MFIBA+ELIC	-16.834	-21.922
MFIBA+Retrained ELIC	-30.373	-32.304
Finetuned MFIBA+Retrained ELIC	-35.992	-38.202

4 Experimental Results and Analysis

4.1 Experimental Settings

We selected the object detection, instance segmentation and keypoint detection as the machine vision tasks, which utilize the multiscale features in decision-making. We randomly selected 2,000 images from the COCO2017 validation dataset to evaluate the compression network. Additionally, considering that the data distribution between natural image datasets and feature map datasets differs, future codecs targeting machine vision may rely on models trained on feature map datasets rather than natural images. We constructed a feature map dataset by randomly selecting 40,000 images from the COCO2017 training dataset. We used the ResNet50-FPN [21] backbone to extract 5-scale features, resulting in 200,000 feature matrices. Each matrix, with 256 channels, was split into 3-channel patches, producing 200,000 3-channel images for retraining the end-to-end feature coding models.

We chose Faster R-CNN [31] as the target network for object detection, which is recommended by the VCM standards group. This network uses ResNet50 [21] backbone extract features at five scales, which collectively contribute to task decision-making. Additionally, to validate the generalizability of the proposed MFIBA on other machine tasks, instance segmentation with Mask R-CNN [20] and keypoint detection with Keypoint R-CNN [13] were used to evaluate the quality of compressed features, respectively. We selected the Efficient Learned Image Compression (ELIC) [19] and as the basic feature codec, on which we applied the proposed MFIBA to improve the feature coding efficiency. We utilized 8 bit rate points from pre-training to establish task loss-rate model. "MFIBA+ELIC" denotes that the proposed MFIBA is applied to ELIC, while "SABA+ELIC" denotes that the SABA [22] is applied to ELIC. "Finetune MFIBA" indicates that the importance weights of features are further calibrated with line search. In addition, since the ELIC was initially proposed for human vision oriented image coding, we retrained ELIC on the feature dataset, which is denoted as "Retrained ELIC". Correspondingly, "MFIBA+Retrained ELIC" and "Finetuned MFIBA+Retrained ELIC" are MFIBA applied to the retrained ELIC and finetuned MFIBA applied to the retrained ELIC. VTM 17.0 is a test model for VVC [4]. To further verify the generalizability of the proposed MFIBA to different codecs, we also applied the MFIBA with the same parameters to another advanced Learned Image Compression Transformer-CNN Mixture (LIC-TCM)[27], labeled as "LIC-TCM".

We used mean average precision with Intersection over Union (IoU) thresholds from 50% to 95% (i.e., mAP@50:95) and 75% (i.e., mAP@75) as evaluation metrics to measure the accuracy of three machine vision tasks, including object detection, instance segmentation and keypoint detection. The feature bit rate is measured with bits per pixel (bpp). The Bjøntegaard-Delta Bit Rate (BDBR) was calculated by comparing with the anchor ELIC [19] and LIC-TCM [27].

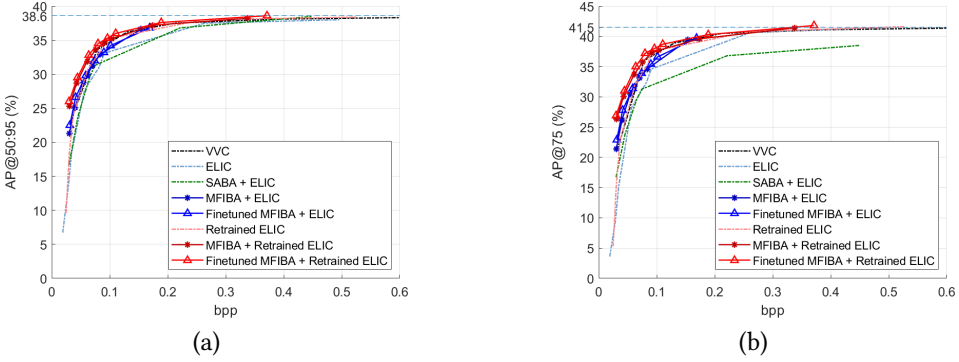


Fig. 8. Coding performance of the Proposed MFIBA based on ELIC for object detection. (a) mAP@50:95 (b) mAP@75.

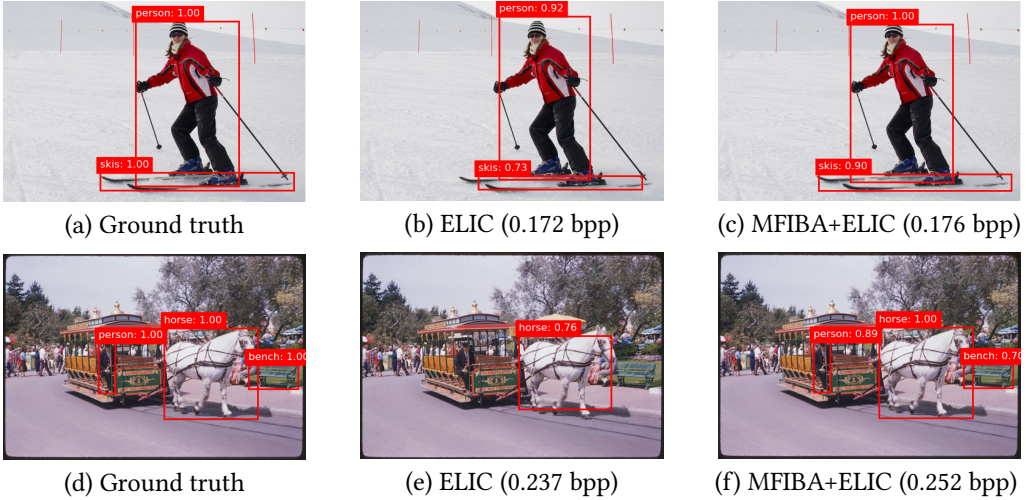


Fig. 9. Visual comparison of object detection using compressed features from different codecs. (a) and (d): Ground truth, (b) and (e): ELIC, (c) and (f): The Proposed MFIBA+ELIC, (a)-(c): image of person and skis, (d)-(f) image of a horse, a person and a bench.

4.2 Compression Performance and Analysis based on ELIC

Table 3 presents quantitative BDBR of the proposed MFIBA on ELIC and benchmark schemes as comparing with the ELIC on object detection. The SABA+ELIC is inferior to pre-trained ELIC with bit rates increasing of 2.113% under mAP@50:95 and 6.073% under the mAP@75 on average. The VTM outperforms the ELIC with 5.661% and 18.625% BDBR gains when task performance is measured with mAP@50:95 and mAP@75, respectively. If ELIC is retained with feature set, 13.477% and 14.179% bit rate saving can be achieved under mAP@50:95 and mAP@75, respectively. It indicates that re-training using feature dataset to transfer LIC of natural images to FCM is somewhat effective. The proposed MFIBA+ELIC achieved bit rate savings of 16.118% under the comprehensive evaluation metric mAP@50:95 and 21.586% under mAP@75. When sufficient computational resources were available, the Finetuned MFIBA+ELIC further improved compression efficiency, and achieved bit

Table 4. BDBR of the proposed MFIBA+LIC-TCM compared to LIC-TCM on object detection. [Unit:%]

Coding schemes	mAP@50:95	mAP@75
SABA [22]+LIC-TCM	-3.572	10.391
VTM 17.0 [4]	-11.818	0.261
MFIBA+LIC-TCM	-18.103	-13.783
Finetuned MFIBA+LIC-TCM	-15.798	-15.374

rate savings of 21.922% bit rate under mAP@75 and 16.834% under mAP@50:95. Based on the retrained ELIC, MFIBA+Retrained ELIC achieved bit rate savings of 30.373% under mAP@50:95 and 32.304% under mAP@75, while the algorithm using the finetuned weights saved bit rate up to 35.992% and 38.202% of the bit rate. Note that the weights of MFIBA used here were from the pre-trained ELIC and were not recalibrated. Fig. 8 illustrates the bit rate allocation results of the ELIC codec, both pre-trained and trained on the feature map training set and the comparison method SABA+ELIC [22] and VTM. It can be observed that the proposed Finetuned MFIBA+Retrained ELIC achieves the best performance and the MFIBA+ELIC significantly outperforms the SABA+ELIC.

These coding results indicate that the proposed MFIBA method significantly enhanced the FCM performance. Also, it can effectively adapt to different learnable deep codecs. Based on the pre-trained ELIC, the Finetuned MFIBA+ELIC slightly outperformed the MFIBA+ELIC. When utilizing the retrained codec, finetuned parameters exhibit stronger generalizability across the retrained encoder compared to MFIBA without finetuning, as the finetuned parameters align more closely with the real importance weights of multiscale features.

In addition to BDBR, Fig. 9 presents the object detection results of two images from COCO2017 dataset whose features were extracted by the original source image, or encoded by ELIC, and MFIBA optimized ELIC and then detected. We can observe from Fig. 9.(b) that the ELIC achieves 0.92 and 0.73 confidence for the person and skis when the coding bit is 0.172 bpp. For the proposed MFIBA optimized ELIC, shown as Fig. 9.(c), it achieves 1.00 and 0.9 confidence, respectively, for the person and skis when the coding bit is 0.176 bpp, which is better and more consistent with the results of the ground truth. Similar results can be found for Fig. 9(d)-(f). Overall, with similar bit rates, the MFIBA optimized ELIC can achieve higher detection accuracy, probability, and confidence compared to the ELIC.

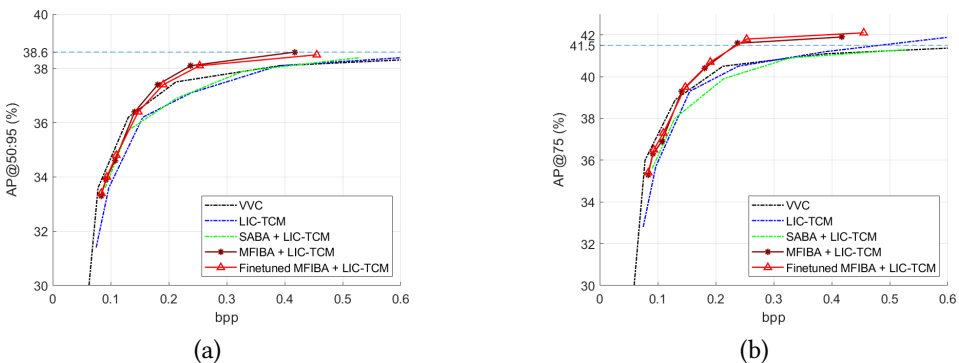


Fig. 10. Coding Performance of the Proposed MFIBA based on LIC-TCM on object detection, (a) mAP@50:95 (b) mAP@75.

Table 5. BDBR of the proposed MFIBA on instance segmentation and keypoint detection, where the accuracy is measured with mAP@50:95 and mAP@75. [Unit:%]

Machine Vision Task	Coding Schemes	mAP@50:95 (+ ELIC)	mAP@50:95 (+ LIC-TCM)	mAP@75 (+ ELIC)	mAP@75 (+ LIC-TCM)
Instance Segmentation	SABA [22]	11.793	13.129	16.141	14.508
	MFIBA	-14.156	-19.588	-20.721	-25.953
	Finetuned MFIBA	-17.212	-19.866	-23.373	-26.799
Keypoint Detection	SABA [22]	8.288	17.523	0.398	18.921
	MFIBA	-34.002	-10.852	-17.029	-4.124
	Finetuned MFIBA	-36.492	-19.597	-16.775	-12.952

4.3 Compression Performance and Analysis based on LIC-TCM

To further validate the performance of the proposed MFIBA, it was applied to another end-to-end image codec, LIC-TCM, to optimize the feature coding efficiency. Similarly to the experimental settings in the previous subsection for the object detection, comparative FCM experiments were performed by applying the proposed MFIBA to the LIC-TCM and compared with the LIC-TCM, VVC, and SABA+LIC-TCM. Note that the parameters we used are calculated from the ELIC codec without updating importance weights. Table 4 presents the quantitative BD-BR comparisons while encoding the deep features, where the original LIC-TCM was used as a reference in calculating BD-BR. We can observe that the SABA+LIC-TCM improves compression performance by saving 3.572% bit rate under mAP@50:95 metric, while the VVC saves an average of 11.818% bit rate but is inferior to LIC-TCM by increasing 0.261% of bit rate under mAP@75. MFIBA+LIC-TCM achieves an average of 18.103% bit rate savings under mAP@50:95 and 13.783% under mAP@75. The Finetuned MFIBA+LIC-TCM saved up to 15.798% of the bit rate under mAP@50:95 and 15.374% under mAP@50:95.

Fig. 10 illustrates FCM results of the proposed MFIBA applied to LIC-TCM, compared with the benchmark coding schemes. It can be observed that the proposed MFIBA+LIC-TCM significantly outperformed the SABA+LIC-TCM and was comparable to VVC at low bit rates while outperforming VVC at high bit rates. The experimental results proved that the proposed MFIBA has good generalizability and can be adapted to different learnable deep codecs. However, the weights of MFIBA finetuned on the ELIC encoder did not improve the encoding performance further as it was applied to the LIC-TCM encoder as compared with the LIC-TCM using the direct MFIBA. This is because the finetuned MFIBA weights are sensitive and potentially correlated with the network structure of the deep encoder. To further improve encoding performance on LIC-TCM, updating the finetuned weights based on the LIC-TCM is preferred. In general, the proposed MFIBA can significantly improve the FCM performance using LIC-TCM.

4.4 Compression Performance and Analysis on Other Machine Vision Tasks

To validate that the proposed MFIBA can adapt to other machine vision tasks, we proposed coding experiments on the instance segmentation and keypoint detection based on ELIC and LIC-TCM. The compression results are shown in Fig. 11 and the quantitative results of BD-BR are shown in Table 5. First, in the instance segmentation, the SABA+ELIC increases BDBR by 11.793% on average compared to the anchor ELIC. The main reason is that SABA was proposed for object detection, but is no longer effective as being applied to instance segmentation directly. Compared to ELIC, the proposed MFIBA+ELIC achieves an average of 14.156% bit rate savings, which is significant. If weights of the MFIBA are calibrated with finetuning, the finetuned MFIBA+ELIC achieves an

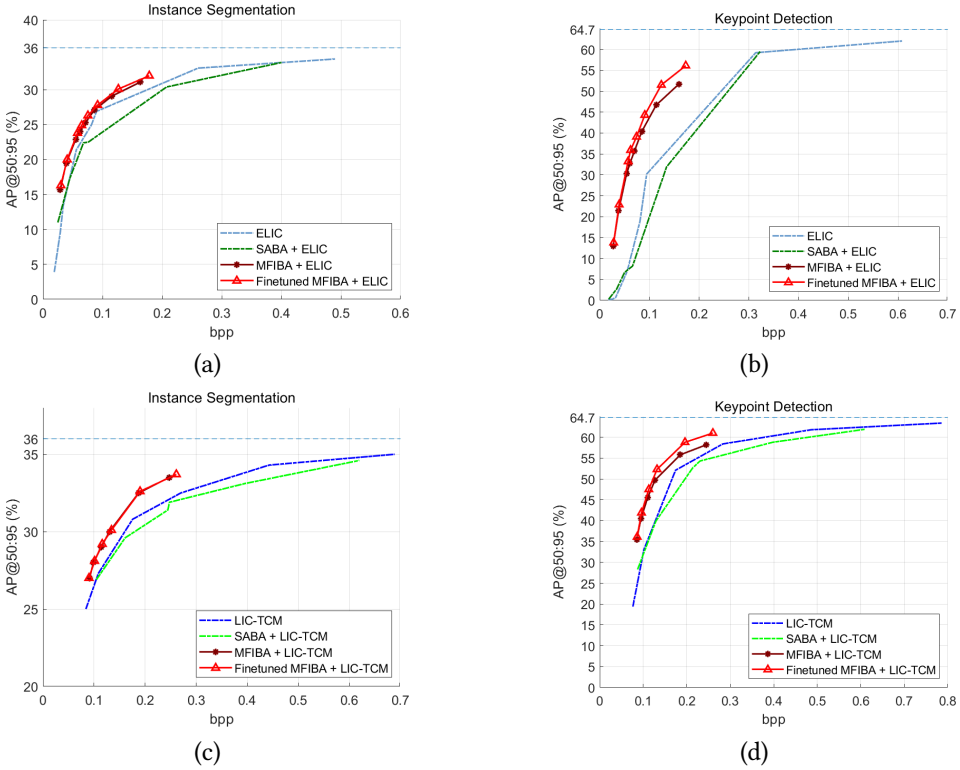


Fig. 11. RD Performance of the proposed MFIBA+ELIC/LIC-TCM on instance segmentation and keypoint detection, where the accuracies are measured with $mAP@50:95$. (a)(c) instance segmentation, (b)(d) keypoint detection, (a)(b) ELIC based, (c)(d) LIC-TCM based.

average of 17.212% bit rate savings. If apply the MFIBA to LIC-TCM, the MFIBA and the Finetuned MFIBA+LIC-TCM achieve an average of 19.588% and 19.866%, respectively. Second, in the keypoint detection, SABA+ELIC increases bit rates by 8.288% compared to the anchor ELIC. The MFIBA and the finetuned MFIBA are able to improve the ELIC and achieve 34.002% and 36.492% BDBR gains on average, respectively. If apply the MFIBA to LIC-TCM, the MFIBA and the finetuned MFIBA achieve 10.852% and 19.597% BDBR gains, respectively. Third, similar results can be found when the accuracies of instance segmentation and keypoint detection are measured with $mAP@75$. In summary, these results show that the proposed MFIBA is generalizable to multiple machine tasks, including instance segmentation and keypoint detection.

4.5 Computational Complexity Analysis

We performed theoretical and experimental analysis on the complexity of the proposed MFIBA. Encoding and decoding experiments were carried out on an Intel Core i9-10900 CPU and a NVIDIA GeForce RTX 3090 GPU. In encoding, the time of precoding multiscale features is denoted as t_{pre} ; the time of estimating importance weights in MFIP and performing bit allocation in the MFIBA algorithm is denoted as t_{assign} . The actual feature coding time is denoted as t_{enc} . In decoding, the decoding time is denoted as t_{dec} , and the time of performing task model for task performance evaluation is denoted as t_{task} . Let m be the number of precoding with different bit rates and $n + 2$

Table 6. Encoding and decoding time of the proposed MFIBA and benchmarks.[Unit:s]

Base codec	Methods	Encoding Time (s)			Decoding Time (s)	
		t_{pre}	t_{assign}	t_{enc}	t_{dec}	t_{task}
ELIC	ELIC	-	-	2.395	1.598	0.394
	SABA[22]+ELIC	6.456	0.001	2.396	1.596	0.396
	MFIBA+ELIC	47.541	0.001	2.403	1.596	0.394
LIC-TCM	LIC-TCM	-	-	2.468	1.646	0.391
	SABA[22]+LIC-TCM	6.581	0.001	2.473	1.651	0.395
	MFIBA+LIC-TCM	24.621	0.001	2.465	1.645	0.388

be the number of different scale features contained in the multiscale features ($i \in 0, 1, \dots, n, P$), then $t_{pre} = m(t_{enc} + t_{dec}) + m(n + 2)t_{task}$. The t_{pre} will be more than m times of $t_{enc} + t_{dec}$.

Table 6 shows encoding and decoding time of the proposed MFIBA and the benchmarks. We have the following five observations. First, t_{pre} of the SABA and MFIBA are 6.456s and 47.541s, respectively. t_{assign} of the SABA and MFIBA are 0.001s, which is negligible. t_{enc} of ELIC, SABA+ELIC and the proposed MFIBA are 2.395s, 2.396s and 2.403s, respectively, which are similar. Second, t_{dec} and t_{task} of the ELIC, SABA+ELIC and MFIBA+ELIC are quite similar as the decoder are generally not changed. Third, similar results can be found for LIC-TCM based coding optimization, where t_{pre} of the MFIBA is 24.621s and higher than that of SABA. Fourth, the t_{pre} based on ELIC is higher than that of t_{pre} based on LIC-TCM. The main reason is the precoding times m are 8 for ELIC and 6 for LIC-TCM, respectively. Higher model accuracy could be achieved with more pre-coding times and task evaluation. Finally, the number of parameters in MFIBA+ELIC and MFIBA+LIC-TCM are 144.65MB and 534.41MB, respectively, which are the same as those of ELIC and LIC-TCM. It means MFIBA generally does not increase the size of model parameter.

5 Conclusions

In this paper, we proposed a Multiscale Feature Importance-based Bit Allocation (MFIBA) for Feature Coding for Machines (FCM), which adaptively allocated coding bits based on the varying importance on different scales of features in machine vision tasks. Firstly, we found that the importance of feature varied with the scales, object size, and image instances and proposed an Multiscale Feature Importance Prediction (MFIP) module to predict feature importance. Secondly, we proposed a task loss-rate model to build the relationship between bit rate and task losses for machine vision tasks. Finally, we developed the MFIBA for end-to-end FCM, where the optimal coding parameters for each scale of feature were calculated by solving a MFIBA optimization function. Experiments demonstrated that the proposed MFIBA can save an average of 21.922% bit rate based on Efficient Learned Image Compression (ELIC) and can achieve an average of 38.201% bit rate saving for codecs retrained on features compared to anchor ELIC. In addition, the MFIBA has good generalizability to different machine vision tasks and base codecs.

References

- [1] Saeed Ranjbar Alvar and Ivan V. Bajić. 2019. Multi-Task Learning with Compressible Features for Collaborative Intelligence. In *2019 IEEE International Conference on Image Processing (ICIP)*. IEEE, Taipei, Taiwan, 1705–1709. <https://doi.org/10.1109/ICIP.2019.8803110>
- [2] João Ascenso, Elena Alshina, and Touradj Ebrahimi. 2023. The JPEG AI Standard: Providing Efficient Human and Machine Visual Data Consumption. *IEEE MultiMedia* 30, 1 (2023), 100–111. <https://doi.org/10.1109/MMUL.2023.3245919>
- [3] Yuanhao Bai, Xu Yang, Xianming Liu, Junjun Jiang, Yaowei Wang, Xiangyang Ji, and Wen Gao. 2021. Towards End-to-End Image Compression and Analysis with Transformers. *ArXiv abs/2112.09300* (2021). <https://api.semanticscholar.org/abs/2112.09300>

org/CorpusID:245329388

- [4] Benjamin Bross, Ye-Kui Wang, Yan Ye, Shan Liu, Jianle Chen, Gary J. Sullivan, and Jens-Rainer Ohm. 2021. Overview of the Versatile Video Coding (VVC) Standard and its Applications. *IEEE Transactions on Circuits and Systems for Video Technology* 31, 10 (2021), 3736–3764. <https://doi.org/10.1109/TCSVT.2021.3101953>
- [5] Lahiru D. Chamain, Fabien Racapé, Jean Bégaint, Akshay Pushparaja, and Simon Feltman. 2021. End-to-End optimized image compression for machines, a study. In *2021 Data Compression Conference (DCC)*. IEEE, Snowbird, UT, USA, 163–172. <https://doi.org/10.1109/DCC50243.2021.00024>
- [6] Yi Chen, Sam Kwong, Mingliang Zhou, Shiqi Wang, Guopu Zhu, and Yi Wang. 2020. Intra Frame Rate Control for Versatile Video Coding with Quadratic Rate-Distortion Modelling. In *ICASSP 2020 - 2020 IEEE International Conference on Acoustics, Speech and Signal Processing (ICASSP)*. 4422–4426. <https://doi.org/10.1109/ICASSP40776.2020.9054633>
- [7] Yi-Hsin Chen, Ying Weng, Chia-Hao Kao, Cheng Chien, Wei-Chen Chiu, and Wenmin Peng. 2023. TransTIC: Transferring Transformer-based Image Compression from Human Perception to Machine Perception. *2023 IEEE/CVF International Conference on Computer Vision (ICCV) (2023)*, 23240–23250. <https://api.semanticscholar.org/CorpusID:259108311>
- [8] Hyomin Choi and Ivan V. Bajić. 2021. Latent-Space Scalability for Multi-Task Collaborative Intelligence. *2021 IEEE International Conference on Image Processing (ICIP) (2021)*, 3562–3566. <https://api.semanticscholar.org/CorpusID:235125754>
- [9] Hyomin Choi and Ivan V. Bajić. 2022. Scalable Image Coding for Humans and Machines. *IEEE Transactions on Image Processing* 31 (2022), 2739–2754. <https://doi.org/10.1109/TIP.2022.3160602>
- [10] Jinyoung Choi and Bohyung Han. 2020. Task-Aware Quantization Network for JPEG Image Compression. In *Computer Vision – ECCV 2020*, Andrea Vedaldi, Horst Bischof, Thomas Brox, and Jan-Michael Frahm (Eds.). Springer International Publishing, Cham, 309–324.
- [11] Felipe Codevilla, Jean-Gabriel Simard, Ross Goroshin, and Christopher Joseph Pal. 2021. Learned Image Compression for Machine Perception. *ArXiv abs/2111.02249 (2021)*. <https://api.semanticscholar.org/CorpusID:241033392>
- [12] Wenxue Cui, Xingtao Wang, Xiaopeng Fan, Shaohui Liu, Xinwei Gao, and Debin Zhao. 2024. Deep Network for Image Compressed Sensing Coding Using Local Structural Sampling. *ACM Trans. Multimedia Comput. Commun. Appl.* 20, 7, Article 212 (May 2024), 22 pages. <https://doi.org/10.1145/3649441>
- [13] Xintao Ding, Qingde Li, Yongqiang Cheng, Jimbao Wang, Weixin Bian, and Biao Jie. 2020. Local keypoint-based Faster R-CNN. *Applied Intelligence* 50 (2020), 3007–3022.
- [14] Lingyu Duan, Jiaying Liu, Wenhan Yang, Tiejun Huang, and Wen Gao. 2020. Video Coding for Machines: A Paradigm of Collaborative Compression and Intelligent Analytics. *IEEE Transactions on Image Processing* 29 (2020), 8680–8695. <https://doi.org/10.1109/TIP.2020.3016485>
- [15] Ling-Yu Duan, Vijay Chandrasekhar, Jie Chen, Jie Lin, Zhe Wang, Tiejun Huang, Bernd Girod, and Wen Gao. 2016. Overview of the MPEG-CDVS Standard. *Trans. Img. Proc.* 25, 1, 179–194. <https://doi.org/10.1109/TIP.2015.2500034>
- [16] Ling-Yu Duan, Yihang Lou, Yan Bai, Tiejun Huang, Wen Gao, Vijay Chandrasekhar, Jie Lin, Shiqi Wang, and Alex Chichung Kot. 2019. Compact Descriptors for Video Analysis: The Emerging MPEG Standard. *IEEE MultiMedia* 26, 2 (2019), 44–54. <https://doi.org/10.1109/MMUL.2018.2873844>
- [17] Ruoyu Feng, Xin Jin, Zongyu Guo, Runsen Feng, Yixin Gao, Tianyu He, Zhizheng Zhang, Simeng Sun, and Zhibo Chen. 2022. Image Coding for Machines with Omnipotent Feature Learning. In *Computer Vision – ECCV 2022*, Shai Avidan, Gabriel Brostow, Moustapha Cissé, Giovanni Maria Farinella, and Tal Hassner (Eds.). Springer Nature Switzerland, Cham, 510–528.
- [18] Wen Gao, Shan Liu, Xiaozhong Xu, Manouchehr Rafie, Yuan Zhang, and Igor D. D. Curcio. 2021. Recent Standard Development Activities on Video Coding for Machines. *ArXiv abs/2105.12653 (2021)*. <https://api.semanticscholar.org/CorpusID:235195868>
- [19] Dailan He, Zi Yang, Weikun Peng, Rui Ma, Hongwei Qin, and Yan Wang. 2022. ELIC: Efficient Learned Image Compression with Unevenly Grouped Space-Channel Contextual Adaptive Coding. *2022 IEEE/CVF Conference on Computer Vision and Pattern Recognition (CVPR) (2022)*, 5708–5717. <https://api.semanticscholar.org/CorpusID:247594672>
- [20] Kaiming He, Georgia Gkioxari, Piotr Dollár, and Ross Girshick. 2017. Mask R-CNN. In *2017 IEEE International Conference on Computer Vision (ICCV)*. IEEE, Venice, Italy, 2980–2988. <https://doi.org/10.1109/ICCV.2017.322>
- [21] Kaiming He, Xiangyu Zhang, Shaoqing Ren, and Jian Sun. 2016. Deep Residual Learning for Image Recognition. In *2016 IEEE Conference on Computer Vision and Pattern Recognition (CVPR)*. IEEE, Las Vegas, NV, USA, 770–778. <https://doi.org/10.1109/CVPR.2016.90>
- [22] Yuzhang Hu, Sifeng Xia, Wenhan Yang, and Jiaying Liu. 2020. Sensitivity-aware bit allocation for intermediate deep feature compression. In *2020 IEEE International Conference on Visual Communications and Image Processing (VCIP)*. IEEE, IEEE, Macau, China, 475–478.
- [23] Zhimeng Huang, Chuanmin Jia, Shanshe Wang, and Siwei Ma. 2021. Visual Analysis Motivated Rate-Distortion Model for Image Coding. In *2021 IEEE International Conference on Multimedia and Expo (ICME)*. IEEE, Shenzhen, China, 1–6. <https://doi.org/10.1109/ICME51207.2021.9428417>

- [24] Nam Le, Honglei Zhang, Francesco Cricri, Ramin Ghaznavi-Youvalari, Hamed Rezazadegan Tavakoli, and Esa Rahtu. 2021. Learned Image Coding for Machines: A Content-Adaptive Approach. In *2021 IEEE International Conference on Multimedia and Expo (ICME)*. IEEE, Shenzhen, China, 1–6. <https://doi.org/10.1109/ICME51207.2021.9428224>
- [25] Tsung-Yi Lin, Priya Goyal, Ross Girshick, Kaiming He, and Piotr Dollár. 2018. Focal Loss for Dense Object Detection. *arXiv:1708.02002*
- [26] Jinming Liu, Heming Sun, and Jiro Katto. 2022. Improving Multiple Machine Vision Tasks in the Compressed Domain. In *2022 26th International Conference on Pattern Recognition (ICPR)*. IEEE, Montreal, QC, Canada, 331–337. <https://doi.org/10.1109/ICPR56361.2022.9956532>
- [27] Jinming Liu, Heming Sun, and Jiro Katto. 2023. Learned Image Compression with Mixed Transformer-CNN Architectures. In *2023 IEEE/CVF Conference on Computer Vision and Pattern Recognition (CVPR)*. IEEE, Vancouver, BC, Canada, 14388–14397. <https://doi.org/10.1109/CVPR52729.2023.01383>
- [28] Kang Liu, Dong Liu, Li Li, Ning Yan, and Houqiang Li. 2021. Semantics-to-Signal Scalable Image Compression with Learned Reversible Representations. *International Journal of Computer Vision* 129 (2021), 2605 – 2621. <https://api.semanticscholar.org/CorpusID:236930362>
- [29] Tie Liu, Mai Xu, Shengxi Li, Chaoran Chen, Li Yang, and Zhuoyi Lv. 2023. Learnt Mutual Feature Compression for Machine Vision. In *ICASSP 2023 - 2023 IEEE International Conference on Acoustics, Speech and Signal Processing (ICASSP)*. IEEE, Rhodes Island, Greece, 1–5. <https://doi.org/10.1109/ICASSP49357.2023.10094830>
- [30] Wen-Hsiao Peng and Hsueh-Ming Hang. 2020. Recent Advances in End-to-End Learned Image and Video Compression. In *2020 IEEE International Conference on Visual Communications and Image Processing (VCIP)*. IEEE, Macau, China, 1–2. <https://doi.org/10.1109/VCIP49819.2020.9301753>
- [31] Shaoqing Ren, Kaiming He, Ross Girshick, and Jian Sun. 2017. Faster R-CNN: Towards Real-Time Object Detection with Region Proposal Networks. *IEEE Transactions on Pattern Analysis and Machine Intelligence* 39, 6 (2017), 1137–1149. <https://doi.org/10.1109/TPAMI.2016.2577031>
- [32] Takahiro Shindo, Kein Yamada, Taiju Watanabe, and Hiroshi Watanabe. 2024. Image Coding for Machines with Edge Information Learning Using Segment Anything. *arXiv preprint arXiv:2403.04173* (2024).
- [33] Hanyue Tu, Li Li, Wengang Zhou, and Houqiang Li. 2024. Reconstruction-free Image Compression for Machine Vision via Knowledge Transfer. *ACM Trans. Multimedia Comput. Commun. Appl.* (July 2024). <https://doi.org/10.1145/3678471> Just Accepted.
- [34] Shurun Wang, Shiqi Wang, Wenhan Yang, Xinfeng Zhang, Shanshe Wang, and Siwei Ma. 2021. Teacher-Student Learning With Multi-Granularity Constraint Towards Compact Facial Feature Representation. In *ICASSP 2021 - 2021 IEEE International Conference on Acoustics, Speech and Signal Processing (ICASSP)*. Institute of Electrical and Electronics Engineers, Inc., United States, 8503–8507. <https://doi.org/10.1109/ICASSP39728.2021.9413506>
- [35] Shurun Wang, Zhao Wang, Shiqi Wang, and Yan Ye. 2021. End-to-End Compression Towards Machine Vision: Network Architecture Design and Optimization. *IEEE Open Journal of Circuits and Systems* 2 (2021), 675–685. <https://doi.org/10.1109/OJCS.2021.3126061>
- [36] Shurun Wang, Zhao Wang, Shiqi Wang, and Yan Ye. 2023. Deep Image Compression Toward Machine Vision: A Unified Optimization Framework. *IEEE Transactions on Circuits and Systems for Video Technology* 33, 6 (2023), 2979–2989. <https://doi.org/10.1109/TCSVT.2022.3230843>
- [37] Zixi Wang, Fan Li, Jing Xu, and Pamela C. Cosman. 2022. Human–Machine Interaction-Oriented Image Coding for Resource-Constrained Visual Monitoring in IoT. *IEEE Internet of Things Journal* 9, 17 (2022), 16181–16195. <https://doi.org/10.1109/JIOT.2022.3150417>
- [38] Ning Yan, Dong Liu, Houqiang Li, and Feng Wu. 2020. Semantically Scalable Image Coding With Compression of Feature Maps. In *2020 IEEE International Conference on Image Processing (ICIP)*. IEEE, Abu Dhabi, United Arab Emirates, 3114–3118. <https://doi.org/10.1109/ICIP40778.2020.9191184>
- [39] Shuai Yang, Yueyu Hu, Wenhan Yang, Ling-Yu Duan, and Jiaying Liu. 2021. Towards Coding for Human and Machine Vision: Scalable Face Image Coding. *IEEE Transactions on Multimedia* 23 (2021), 2957–2971. <https://doi.org/10.1109/TMM.2021.3068580>
- [40] Wenhan Yang, Haofeng Huang, Yueyu Hu, Ling-Yu Duan, and Jiaying Liu. 2024. Video Coding for Machines: Compact Visual Representation Compression for Intelligent Collaborative Analytics. *IEEE Transactions on Pattern Analysis and Machine Intelligence* 46, 7 (2024), 5174–5191. <https://doi.org/10.1109/TPAMI.2024.3367293>
- [41] Hui Yuan, Sam Kwong, Xu Wang, Wei Gao, and Yun Zhang. 2015. Rate Distortion Optimized Inter-View Frame Level Bit Allocation Method for MV-HEVC. *IEEE Transactions on Multimedia* 17, 12 (2015), 2134–2146. <https://doi.org/10.1109/TMM.2015.2477682>
- [42] Gai Zhang, Xinfeng Zhang, and Lv Tang. 2024. Unified and Scalable Deep Image Compression Framework for Human and Machine. *ACM Trans. Multimedia Comput. Commun. Appl.* (July 2024). <https://doi.org/10.1145/3678472> Just Accepted.

- [43] Pingping Zhang, Shiqi Wang, Meng Wang, Jiguo Li, Xu Wang, and Sam Kwong. 2023. Rethinking semantic image compression: Scalable representation with cross-modality transfer. *IEEE Transactions on circuits and systems for video technology* 33, 8 (2023), 4441–4445.
- [44] Yun Zhang, Haoqin Lin, Jing Sun, Linwei Zhu, and Sam Kwong. 2024. Learning to Predict Object-Wise Just Recognizable Distortion for Image and Video Compression. *IEEE Transactions on Multimedia* 26 (2024), 5925–5938. <https://doi.org/10.1109/TMM.2023.3340882>
- [45] Ezgi Özyilkan, Mateen Ulhaq, Hyomin Choi, and Fabien Racadé. 2023. Learned Disentangled Latent Representations for Scalable Image Coding for Humans and Machines. In *2023 Data Compression Conference (DCC)*. IEEE, Snowbird, UT, USA, 42–51. <https://doi.org/10.1109/DCC55655.2023.00012>